Correlation between wettability and dissolution of Calcite

Mariam AlMahri,[a†] Jin-You Lu [b†], Shih-Wen Chen d, Tuza Olukan [e], Thomas Chung-Kuang Yang [f], Saeed Alhassan [a] and Matteo Chiesa [c,e*]

a. Department of Chemical Engineering, Khalifa University of Science and Technology, PO Box 127788, Abu Dhabi, United Arab Emirates

b. Advanced Materials Research Centre, Technology Innovation Institute, Abu Dhabi, United Arab Emirates.

c. Laboratory for Energy and NanoScience, Khalifa University of Science and Technology, Masdar Campus, Abu Dhabi, United Arab Emirates.

d. Graduate Institute of Automation Technology, National Taipei University of Technology, Taipei, Taiwan.

e. Department of Physics and Technology, UiT The Arctic University of Norway, Tromsø, Norway.

f. Department of Chemical Engineering and Biotechnology, National Taipei University of Technology, Taipei, Taiwan.

† Equally contributing Authors

* Corresponding author

ABSTRACT: Calcite, a prevalent mineral in the earth's crust, plays a pivotal role in various geological and industrial processes, including carbon sequestration, water treatment, and enhanced oil recovery. Understanding how wettability—a crucial surface property influenced by the interaction between calcite and surrounding fluids—affects calcite's dissolution is essential for optimizing these processes. We conducted a series of experiments to study the wettability and its relation to calcite dissolution of atomically flat calcite surface under deionized water. This system provides a simple environment that allow us to study the wettability alteration in the absence of external ions except the one generated during the dissolution process. Using macroscopic, microscopic, and nanoscopic analytical techniques, we observed that surface evolution progresses from the initial formation of chemical heterogeneities to the gradual growth of a surface water layer strongly bonded to the calcite surface on the timescale of hours as the system reaches an equilibrium state. We also show that the surface evolution is directly related to the calcite dissolution and it depends on the degree of solution saturation. This research not only sheds light on fundamental aspects of calcite behavior in aqueous solutions but also establishes a foundation for future studies aiming to manipulate mineral surfaces for enhanced performance in their respective applications.

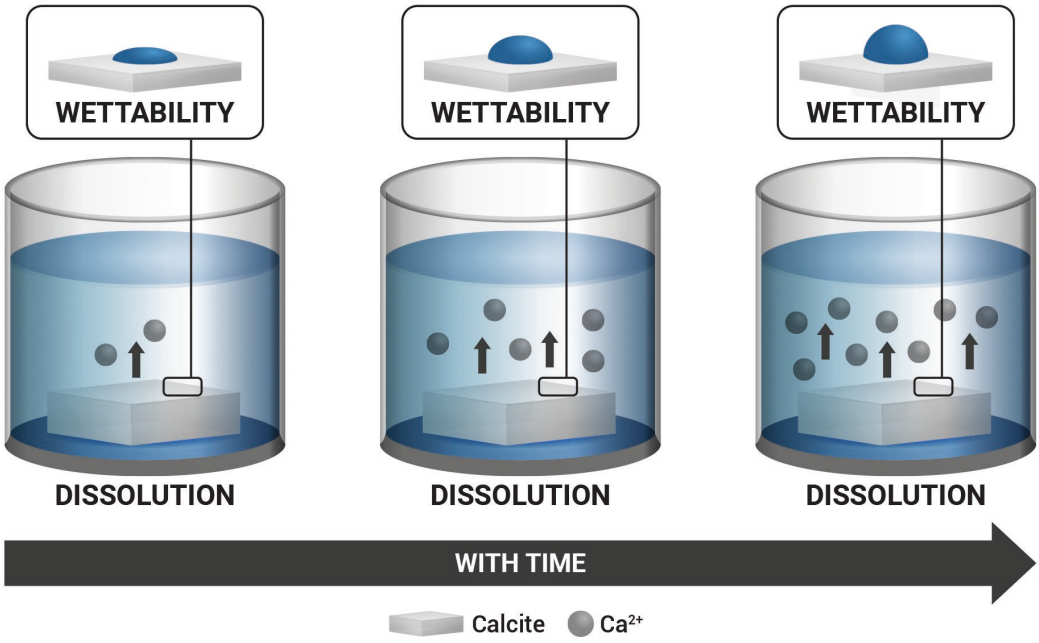

Introduction

Understanding the complex interactions between minerals and fluids is crucial for advancing a multitude of scientific and industrial processes. Among these minerals, calcite, a naturally occurring form of calcium carbonate ($CaCO_3$), occupies a prominent position due to its abundance in the earth's crust and its critical role in various geological and industrial applications. These interactions are key to understanding phenomena such as karst landscape formation[1], atmospheric CO_2 sequestration[2], and enhancing oil recovery from subsurface reservoirs. At the heart of these processes lies wettability — the measure of a liquid's capacity to maintain contact with a solid surface, which significantly influences the efficiency of oil recovery and other fluid-mineral interactions [3-7]. Despite the well-acknowledged importance of wettability, the mechanisms behind its alteration, particularly in the context of oil recovery from carbonate rocks using low salinity or ionic-modified water injections, remain incompletely understood[8-14]. The complexity arises from the multitude of factors at play, including thermodynamic conditions, rock mineralogy, and the interactions with crude oil's acidic and basic components. A deeper exploration into these aspects is essential, necessitating a decoupling of the rock's physical morphology from its chemical composition to unravel the intricacies of wettability alteration mechanisms[15].

Research has increasingly highlighted the impact of water chemistry on the physical and chemical properties of calcite. Studies have shown that alterations in surface wettability, prompted by changes in water ions, could lead to variations in calcite's dissolution rates and patterns, potentially impacting a wide range of applications beyond oil recovery[16-18]. The study of mineral interactions in liquid systems, both with and without external ions, requires careful consideration of dissolution and growth mechanisms. The dissolution of calcite, fundamental to understanding these interactions, is represented by the reaction[19]:

$$CaCO_3(s) \Leftrightarrow Ca^{2+}(aq) + {CO_3}^{2-}(aq) \qquad (1)$$

The intricacies of wettability and its relationship with calcite dissolution in various aqueous environments have captivated researchers across multiple disciplines. A seminal work by Zhang et al. revealed that the presence of divalent cations could notably enhance the dissolution rate of calcite by modifying the surface charge and facilitating the adsorption of water molecules[20]. This finding underscores the importance of specific ion effects on calcite's surface properties and dissolution behaviour. Conversely, J Wang et al. presented findings that calcite dissolution controlled the surface charge and showed that the ionic strength plays a significant role in the diffusion double layer, potentially changing the wettability of calcite surfaces[21]. Their work contributes to a nuanced understanding of how electrolyte concentration influences mineral surface interactions. The role of ion-free water, such as deionized (DI) water, in modulating calcite's wettability and dissolution has, however, been less explored. Early insights by James L et al. suggested that the absence of ions could influence the hydrophobicity of mineral surfaces, proposing that DI water might induce unique interfacial phenomena due to its high surface tension and the absence of screening ions[22]. More recently, Rao et al. explored the microscale interactions between DI water and calcite, suggesting potential alterations in dissolution dynamics driven by changes in surface energy and hydration layers[23].

Despite these contributions, a comprehensive understanding of how ion-free water specifically impacts the wettability and dissolution of calcite is still lacking. The literature indicates a need for systematic studies that isolate the effects of deionized water from other influencing factors, such as pH adjustments and the presence of organic matter. To address this gap, this study aims to meticulously examine the influence of ion-free water (DI water) on calcite wettability interactions and its correlation with the dissolution process. By focusing on the unique environment presented by DI water, this research seeks to uncover the fundamental mechanisms driving these interactions. Employing a suite of advanced analytical techniques, this investigation will delve into the nuances of the calcite-water interface, aiming to provide new insights into a field ripe for discovery

Several characterization tools have been employed for the investigation of calcite surfaces in solutions with different compositions. For instance, electrophoretic mobility measurements of zeta potential on calcite surfaces in aqueous solutions describe ion distribution at the interface between calcite and water[24, 25]. Potentiometric titration has been used to study key reactions, such as dissolution and precipitation of the calcite crystals[26]. Atomic force microscopy (AFM) studies on mineral rocks in solution provide information about interaction and adhesive forces between rock surfaces and molecules[27, 28]. Despite the importance of these investigation tools, the measurement results are prone to be affected by slight changes of the sample conditions, such as time span in the solution, concentration, and composition of the ions. In a previous study we have shown that the calcite sample preparation techniques influence the overall macroscopic static water contact angle (WCA) and microscopic atomic force microscopy (AFM) measurements[29]. We showed that a thin film of water is presented on the calcite surface after aging, and that this water affects the overall results causing a misleading increase in the force of adhesion (surface energy) and consequently a reduction in the absolute value of the contact angle. We further demonstrate that freeze-drying is a suitable technique that can be used to remove this water layer to obtain a reliable quantitative measure of calcite surface wettability alteration. In this study, we follow the same technique and we use freeze-drying before characterizing the samples.

Here, we utilized our experimental setup that includes macroscopic, microscopic and nanoscopic techniques, to examine the wettability of calcite upon exposure to Deionized (DI) water and we relate that to the dissolution mechanism. The multi-scale investigation of wettability alteration and dissolution allow for a deeper understanding of the relationship between processes observed at the atomic

scale and their bulk, phenomenological expression. This includes, static water contact angle (WCA) measurements, atomic force microscopy (AFM), X-ray photoelectron spectroscopy (XPS) and Fourier-transform infrared spectroscopy (FTIR) at various aging time. We also use Ion Chromatography to measure the Ca^{2+} ion concentrations at various aging times to represent the dissolution of calcite. It is important to emphasise that we are not trying to calculate the rate of dissolution of calcite but rather connecting it to the wettability alteration in absence of external ions. Moreover, Density functional theory simulations are employed to investigate the calcite/water interface in the atomic scale, something that allows us to link experimental characterizations with intrinsic wettability alternation due to the bound water layer[30]. This work contributes to the broader understanding of mineral-fluid interactions by focusing on a system simplified to its most fundamental constituents: calcite and ion-free water. Through this lens, we explore the nuanced ways in which the absence of ions can alter surface wettability and its relation to the dissolution dynamics, providing a foundation for future studies and technological advancements in fields as diverse as geology, environmental science, and enhanced oil recovery.

Experimental section

Calcite Sample Preparation

Samples were prepared from calcite stocks (single crystal, optical quality, Iceland spar variety, cleavage plane of ($10\bar{1}4$). The Crystallographic orientation was confirmed by XRD performed using an XRD PANalytical Empyrean. A single peak at ≈29.51° was obtained, which corresponds to the ($10\bar{1}4$) cleavage plane (see Figure S1) [31]. Calcite samples of 2×2 cm were mechanically cleaved along the ($10\bar{1}4$) cleavage plane with a small hammer. Care was taken to avoid environmental contamination during the process, samples were immediately placed in a sealed flask (100 ml) containing DI water to age. After aging, the samples were taken out of the solution and the remaining water on the crystal surface was removed using freeze-drying technique before characterization by WCA, AFM, XPS, and FTIR. The remaining solutions where the samples aged, were analysed by Ion Chromatography to quantify the number of dissolved calcium ions (Refer to Figure 1).

During the freeze-drying, the samples were dried using FreeZone -105° C 4.5 Litre Cascade Benchtop Freeze Dry System. During the freeze-drying, the samples were frozen in a shell-freezer for 24 hours then placed in a FreeZone -105° C 4.5 Litre Cascade Benchtop Freeze Dry System for another 24 hours. The samples were then removed from the chamber in the freeze-drying system and placed in a desiccator to prevent atmospheric moisture accumulation on their surface. For consistency, all WCA, AFM, XPS, and FTIR measurements were taken within one hour from the time of removing the samples from the freeze-dryer.

In our experiments, the samples were not polished in order to better represent the naturally porous and heterogeneous reservoir rock system. Stipp et al. [32] showed in fact that polished calcite samples, even with quite fine grit, are rougher than non-polished samples.

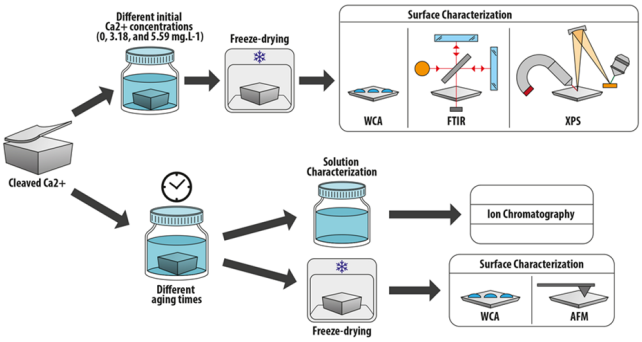

Figure 1 Experimental set up and characterization techniques

Static water contact angle (WCA) measurements

The WCA measurements were obtained with a Kyowa DM-701 contact angle machine under ambient conditions, and elaborated with FAMAS (interFAce Measurement & Analysis System), the software provided by Kyowa. WCAs were measured by depositing water droplets of 0.8 mL on the calcite surface. The contact angle measurements were taken after different aging times, ranging between 0 hours, i.e., freshly cleaved, and 0.5, 1, 3, 6, 9, 12 and 24 hours. Aging was performed by immersing the samples in DI water at 22 ± 2 °C. For each time step, a different calcite crystal was used and an average WCA values and standard deviations were calculated over at least 10 measurements. Experiments were repeated at least three times to ensure reproducibility.

Ion Chromatography System Dionex ICS-5000

In order to quantify the time evolution of the number of dissolved calcium ions in solution, the solutions were analysed by ion chromatography System Dionex ICS-5000 (IC). This system includes a Dionex AS20 Column, a conductivity detector with a detection limit to Ca^{2+} of approximately 50 ppb (parts per billion by mass) and an autosampler (all supplied by Thermo Scientific). The eluent used was KOH (Dionex EGC III KOH, ACS grade), and it passed through the columns at a flow rate of 1.0 mL/min with a concentration gradient. The IC system was calibrated using a certified standard solution (Sigma Aldrich) containing 10 ppm of Li^+, Na^+, K^+, Ca^{2+}, and Mg^{2+} with an uncertainty of less than 0.02 ppm. The water samples were first diluted and then placed in an auto-sampler from which several injections were made onto the IC column.

Atomic Force Microscope (AFM) Force Spectroscopy Measurements

Calcite samples were scanned with a Cypher AFM from Asylum Research using standard OLYMPUS cantilevers (AC160TS) with k ≈ 40 N/m, Q ≈ 500, and f 0 ≈ 300 kHz.

The AFM was operated in the amplitude modulation (AM) mode for both image scanning and force measuring. The force reconstruction method uses the Sader–Jarvis–Katan formalism, where the force is reconstructed by considering variations in amplitude and phase as a function of tip-sample separation distance d. Amplitude-phase-distance (APD) curves were acquired for each time step. Moreover, since it is known that the tip radius (R) can have a great effect on the interaction force between the tip and the surface, it was continuously monitored in situ with the critical amplitude method to ensure that R remained constant during the experiment [33]. A total of 100 APD curves were collected on the calcite surface and the standard deviations were calculated for each time step taken on calcite.

Fourier-transform infrared spectroscopy (FTIR) measurements

Three samples were soaked individually in pure DI water, DI water with 3.18 $mg.L^{-1}$ of calcium carbonate, and DI water with 5.59 $mg.L^{-1}$ of calcium carbonate, respectively. After the freeze-drying process is complete, we put calcite samples on the attenuated total reflectance stage for obtaining their infrared spectrum by Spotlight 200i Sp2, Perkin-Elmer. The resolution of the spectrometer was 4 cm^{-1}, and the wavenumber ranged from 4000 cm^{-1} to 400 cm^{-1}. For better normalizations of all scan data with a background calibration, SingleBeam scan mode was selected with 64 accumulation times. The presented FTIR spectra are respectively normalized to 2514 cm^{-1} of calcite absorption peak [34].

X-ray photoelectron spectroscopy (XPS)

After collecting the FTIR signals, all three samples were characterized by X-ray photoelectron spectroscopy (XPS, JEOL, JPS-9030, Japan). Following similar sample preparation techniques as those used for FTIR measurements, we further investigate the calcite surface at the nanoscale using XPS spectroscopy, which is a more surface-sensitive spectroscopic technique and that allows us to measure the elemental composition of the chemical state on the calcite surface. First, the sample holder was cleaned using 98% ethanol and put into the vacuum chamber, which was evacuated to an ultra-high vacuum state ($7x10^{-8}$ Pa). A standard Mg Kα radiation source (1253.6 eV) was used to record the wide and narrow XPS spectra. All samples' spectra were calibrated with the binding energy of carbon C1s (C-C, C-H) peak of 284.8 eV as the reference. To analyse water adhesion, oxygen O1s peak was added to the quantitative measurement ranging from 519.17eV to 539.17eV.

Quantum Molecular Dynamics (MD) simulations.

All Quantum MD simulations are performed using the Quantum Espresso package [35]. The calcite (10.4) surface is represented by four layers of $CaCO_3$ units with $10.031 \times 8.113 Å^2$ surface area. The bottom layer is fixed as the bulk calcite. The parameter settings are the same as the DFT energy calculations except for the kinetic energy and density cut offs, which are set as 25 and 250 Ry, respectively. The 1 × 1 × 1 Monkhorst-Pack k-point mesh is used for all the total energy calculations. The Berendsen thermostat [36] is used to re-scale the velocities of atoms in Quantum MD simulation to control the system temperature and each time step in the Quantum MD simulation is 0.96756 femtosecond. The simulations are conducted with a constant temperature of 900K, constant volume (NVT) ensemble. The 1 × 1 × 1 Monkhorst-Pack k-point mesh is used for all the QMD calculations. In this work, our ideal system just contains 4 calcium ions in 32 water molecules (96 atoms) on the calcite crystal surface. There were 80 atoms of four calcite layers composed of Ca^{2+} and CO_3^{2-} ions. In order to reach an equilibrium state, the system has been continuously annealing for 4.5 ps with a time step of 1 fs.

Plane-wave density functional theory calculations.

All DFT simulations for total energy calculations were performed using the Quantum Espresso package. The Perdew Burke Ernzerhof (PBE) functional in generalized gradient approximations [37] (GGA) is used for the exchange-correlation energy with the ultrasoft pseudo-potentials [38]. For van der Waals corrections, the DFT-D2 method of Grimme [39] is applied to DFT simulations. The kinetic energy cutoffs and density cutoffs of DFT simulations are set as 35 and 350 Ry, respectively, which give the converged adhesion energies for multilayer of water on the calcite surface. The 2 × 2 × 1 Monkhorst-Pack k-point mesh is used for all the total energy calculations. The criterion for the geometry optimization is met once the total energy is less than $1x10^{-4}$ Ry and the interatomic force is less than $1x10^{-3}$ Ry/Bohr.

Results and Discussion

Macroscopic measurements to evaluate the wettability of calcite after different aging times in DI water were first carried out with water contact angle (WCA) sessile drop method. After their respective aging time, calcite samples were removed from the DI water and dried by Freeze-drying before WCA measurements. With consideration to the random error in the experimental measurements, the contact angle over 24 hours aging period is shown in Figure-2(a). The WCA of the calcite surface increases with increasing the aging times in DI water. Specifically, the WCA exhibits a sharp transition from 5° super-hydrophilic surface (Freshly cleaved) to 93° ± 6.4° within 3 hours upon aging in DI water. The measured contact angle remains somehow constant for the next 21 hours. The wettability transition suggests that the surface energy of the calcite crystal surface decreased with the increasing aging time in DI water. At the macroscopic scale, specifically when utilizing the WCA method, it proves challenging to definitively determine whether the shift in wettability over time can be attributed to changes in morphology or chemistry. Nevertheless, AFM measurements offer the capability to separate these effects, providing clarity to the WCA results. AFM measurements were carried out to investigate

the reason behind the decrease of surface energy during the first three hours. The root-mean-square (RMS) roughness value of the calcites from the topography map (Figure S3 in Supporting information) was computed for samples aged at different times. The comparison of RMS roughness between freshly cleaved conditions and those after 24 hours of exposure reveals a mere 240 pm difference, indicating that any morphological alterations are minimal and unlikely to be the cause of such a change in wettability.

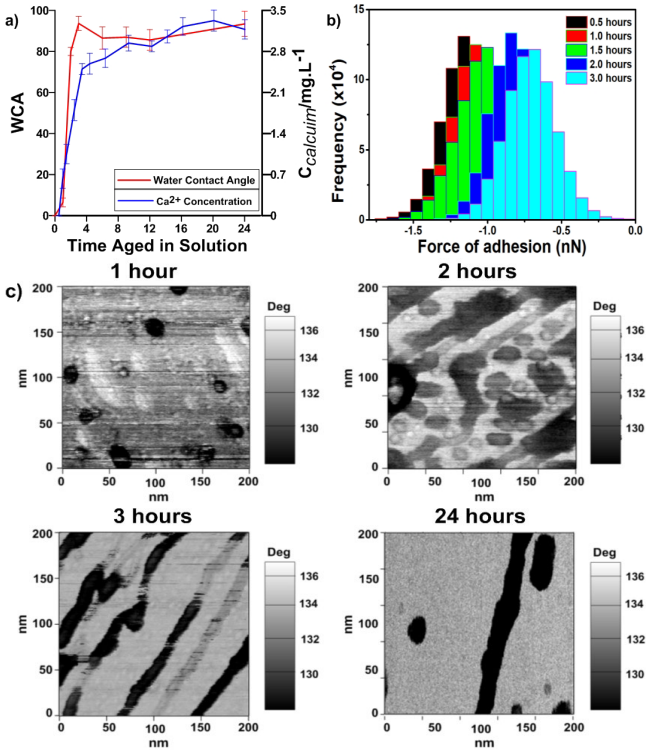

Figure 2 a) WCA measurement of freeze-dried calcite surface, where the samples have been aged in DI water for different time spans. The measured Ca^{+2} ion concentration of the solution, where we immerse the freshly-cleaved calcite crystal in, over 24 hours using ion chromatography. b) Histogram representation of the force maps obtained by AFM of calcite aged in DI water at different aging times (0.5, 1, 1.5, 2 and 3). c) AFM phase images of freeze-dried calcite surface at aging times (1, 2, 3 and 24 hours).

AFM phase imaging, providing insights into the surface chemical composition, revealed contrasts in Figure 2(c) illustrating the calcite surface at different aging times in DI water. The observed contrasts suggest variations in energy dissipation across the surface, qualitatively interpreted as surface chemical heterogeneity resulting from exposure to DI water [40]. In the initial 1-2 hours, the phase images display random patches of coarse contrasting features, commonly known as etch pits. While the literature describes these etch pits as nonmetric morphological features, our AFM phase images indicate that these etch pits reveal a chemical alteration not previously mentioned in the literature [27, 41, 42]. MacInnis and Brantley (1993) studied the development of etch pits on dissolved calcite over time [43]. They demonstrated that the etch pits nucleate soon after the calcite comes into contact with water at all available sites on the initially cleaved surface. This phenomenon is evident in the phase images in Figure 2(c), where the pits increase in size with time in the water. Beyond three hours of aging time, the growing etch pits intersect, resulting in a relatively homogeneous surface. This indicates the formation of a new chemically altered material covering the calcite surface when the system reaches a stable equilibrium state.

Force of adhesion distributions obtained from bimodal AFM scanning [44-46] in repulsive regime allows the possibility of tracking back the aging process quantitatively. The magnitude of The force of adhesion F_{AD} depends on the AFM tip radius and sample surface chemistry, and can be expressed as shown in the expression [47] below.

$$F_{AD} = \frac{R_{tip}H}{6a_0^2} \quad (2)$$

Where R_{tip} the radius of the AFM is tip, H is the Hamaker constant, and a_0 is the intermolecular distance.

The force of adhesion distributions at different aging times are reported in Figure 2(b) where one can observe how the mean attractive force on the calcite surface is rapidly decreasing during the first three hours. After that, the measured F_{AD} is nearly the same as that obtained on the three hours-aged samples and therefore not visible in the graph. The force of adhesion map of the calcite surfaces at different time spans can be found in Figure S4 of Supporting Information. Since R_{tip} remained under constant monitoring throughout the experiments to ensure stability, the variations in F_{AD} can be attributed exclusively to the properties of the sample's surface[15]. In other words, the two phases present on the calcite surfaces are chemically different. AFM force measurements are in agreement with AFM phase images and WCA measurements which shows that when freshly cleaved calcite aged in DI water, chemistry heterogeneity develops and consequently changes the surface energy.

Turning our attention to the opposite end of the process, which is the DI water solution. The most straightforward method for assessing calcite dissolution is by tracking the concentration of calcium ions (Ca^{2+}) as it changes over time. In Figure 2(a), the blue line shows that Ca^{2+} ions rapidly increase in the first three hours and stabilize during the following 21 hours. The time-evolution of the Ca^{2+} ion concentration in the solution is observed to be parallel to that of the WCA on the freeze-dried calcite surfaces. However, the rate of change in the Ca^{2+} ion concentration is more gradual and demonstrates lesser sensitivity to surface roughness compared to the WCA, attributable to their distinct underlying mechanisms. For any interfacial reaction, the rate of the surface reaction can be influenced by either the reaction occurring at the surface itself or by the mass transport of material to and from the interface[48]. In the case of calcite, it has long been understood that the dissolution rates of calcite are dictated by diffusion-controlled mechanisms at pH levels below 3.5, while surface-controlled mechanisms come into play at pH levels exceeding 3.5 [49]. Accordingly, when calcite dissolves in acidic solutions and the dissolution rate operates according to a diffusion-controlled mechanism, the rupture of chemical

bonds and subsequent detachment of molecules from the mineral surface is faster than the diffusion of reaction products through the mineral-water interface. However, in the higher pH region, the dissolution rate is governed by surface-controlled processes and the dissolution rate becomes heavily dependent on the surface topography and population of various reactive surface sites. Hence dissolution in the higher pH region is more dependent upon solution chemistry. In our experiments, we measured the initial pH of the deionized water to be between 6.6-6.8. We anticipate the pH to slightly rise as a result of calcite dissolution, thereby situating the dissolution rate within a surface-controlled regime which depends on the solution chemistry ie. the degree of solution saturation.

Equation 3 below is the prevalent formula employed to describe mineral dissolution processes, where R represents the dissolution rate, k is the rate constant governing the dissolution process, Ω represents the saturation state relative to the specific mineral in consideration, and n is the reaction order.

$$\boldsymbol{R = k(1-\Omega)^n} \quad (3)$$

Equation 3 suggests that mineral dissolution rates exhibit a direct correlation with solution undersaturation. This implies that the dissolution process is more favourable under lower saturation conditions (< 1), but less favourable when saturation states are higher (> 1). Xu et al. have observed a similar phenomenon in the conte xt of calcite dissolution, where dissolution rates decrease with increasing Ω, following a non-linear pattern. It's essential to emphasize that our objective is not to calculate the rate of calcite dissolution, but rather to establish a connection between dissolution and wettability alteration. To investigate the impact of undersaturation on the wettability of the calcite surface, we immersed a 24-hour-aged calcite crystal in a fresh DI water solution. Water contact angle (WCA) measurements were conducted as depicted in Figure 3. The results indicate that when the aged calcite crystal (WCA ≈ 90), as shown in Figure 2(a), is removed from its solution and placed in fresh DI water, the calcite surface quickly reverts to a hydrophilic state (WCA ≈ 0) within just 30 minutes (as shown in the inset graph). This is likely attributed to the non-equilibrium condition on the calcite surface caused by the undersaturation and the initiation of the dissolution process once again. Keeping the crystal in the DI water for several hours, causes the WCA to increase and returns to the constant value of nearly 90 degrees, this behaviour closely mirrors the process observed when a freshly cleaved calcite crystal is placed in DI water. Furthermore, both the aged and freshly cleaved calcite surfaces lead to solutions reaching the identical ionic concentration of ≈ 3.1 Ca^{2+}/mg/L. This observation suggests that the wettability of the calcite surface in the solution is dependent upon the concentration of calcium ions and, by extension, the rate of calcite dissolution.

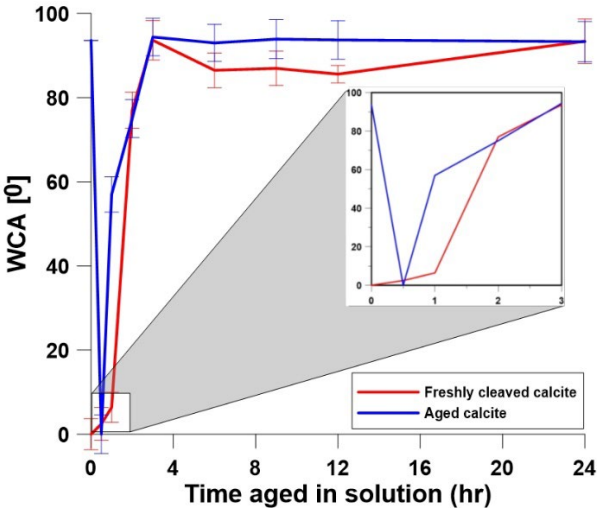

Figure 3 WCA of freshly cleaved and 24-hours aged calcite in the DI water, where the samples have been characterized after freeze-drying techniques. The inset graph focuses on the drop of the aged calcite.

To further investigate and compare the dependence of the calcite surface wettability on the concentration of calcium ions we immerse a freshly cleaved calcite crystal in three solutions with different initial Ca^{2+} concentrations of 0 $mg.L^{-1}$ (DI water), 3 $mg.L^{-1}$ and 5 $mg.L^{-1}$. After immersing the samples in solution for 24 hours, the measured Ca^{2+} ion concentration reaches constant values of 3.18 $mg.L^{-1}$ for calcite aged in DI water , 5.29 $mg.L^{-1}$ for calcite aged in 3 $mg.L^{-1}$ solution and 6.45 $mg.L^{-1}$ for calcite aged in 5 $mg.L^{-1}$ solutions. Each experiment was repeated at least three times to ensure reproducibility. Figure 4 shows that the WCA of calcite surface decreases as the concentration of Ca^{2+} ions in the solution increases. This phenomenon is attributed to the slowing down of the initiation and progression of dissolution as the ion concentration rises. The reduced dissolution rates have resulted in the surface retaining its initial high surface energy, leading to a clear indication of the correlation between calcite dissolution and alterations in its surface wettability. Where the Ca^{2+} ions concentration plays a major role in the dissolution process and by extension the surface energy.

Figures-2 and 4 indicate that the water-wetness of calcite surface is strongly tied to the rate of calcite dissolution and the degree of water saturation. In instances of high saturation with Ca2+ ions, the dissolution reactions occur at a slower pace, resulting in minimal changes to surface wettability. Conversely, at lower saturation levels, the dissolution process accelerates, leading to significant alterations in surface wettability. Whether the wettability alteration leans more towards becoming water-wet or not depends on the state of surface equilibrium. If the saturation decreases after reaching equilibrium, dissolution resumes, causing surface energy to rise until a new equilibrium is achieved. However, if the saturation decreases before surface equilibrium is established, surface energy decreases, ultimately leading to the establishment of an equilibrium state between the solution and the calcite surface.

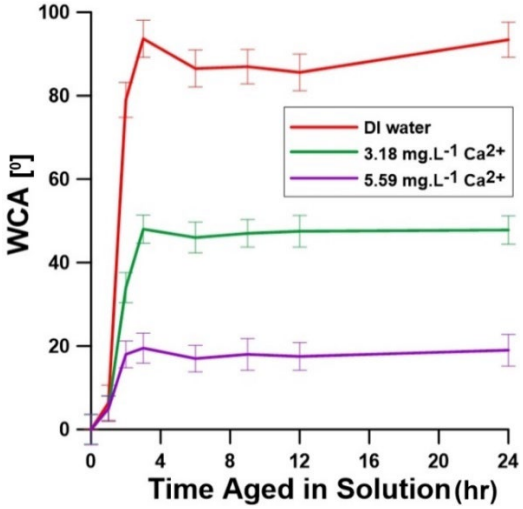

Figure 4 WCA of calcite surface under three solutions with different initial Ca^{2+} concentrations of 0, 3.18, and 5.59 $mg.L^{-1}$.

FTIR characterization on the freeze-dried calcite surfaces were used to investigate what kind of composition causes the calcite surface wettability alteration. In Figure 5a, the FTIR spectra show a broad absorption OH peak at 3400 cm^{-1} and two sharp absorption C-H peaks at 2924 cm^{-1} and 2852 cm^{-1}. It should be noted that the OH-peak just appears under low Ca^{2+} concentration, which indicates that there is a significant amount of water molecules strongly adhere to the calcite surface and cannot be removed by freeze-drying. These water molecules, as the proposed stern layer in the Gouy-Chapman–Stern model strongly bound to the charged surface, effectively screens the polar interaction of the calcite surface and cause the calcite surface to be hydrophobic [50]. As the Ca^{2+} ion concentration increases, the water signal nearly disappears in the spectra. This can be attributed to the deceleration of the dissolution process due to the increased presence of Ca^{2+} ions, as previously discussed. Which in turn leads to a low wetting alteration of the surface. Consequently, the water signal experiences a significant reduction beyond the measurement resolution.

Figure 5(b)&(d) show two peaks in the O_{1s} spectrum. The major peak is the signal from the bulk oxide (calcite), and the other smaller one at 533 eV corresponds to an H_2O signal. As the Ca^{2+} ion concentration of the solution is increased, the relative intensity H_2O of the freeze-dried calcite surface is decreased. The intensity of CO_3 binding in the XPS spectra is nearly the same for solutions with different Ca^{2+} ion concentrations, which proves the efficacy of the XPS measurement. The stronger intensity of H_2O at the lower Ca^{2+} concentration possibly indicates a thicker of water layer on freeze-dried calcite surface, which causes the chemistry of the calcite surface to change. In the combination of WCA, AFM, and XPS characterization results with our density functional theory simulation, our studies give evidence that the stern layer on the calcite surface is very sensitive to the Ca^{2+} ion concentration, which in turn determines the calcite surface wettability in the solution. Our work also agrees with the reported dependence of the stern layer thickness at the silica/ electrolyte interface on the ion concentration of the electrolyte [51].

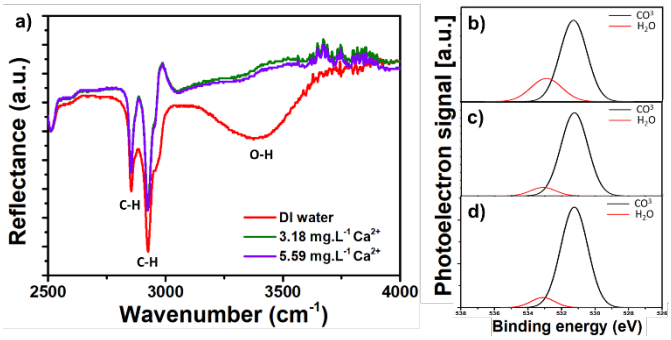

Figure 5 a) FTIR spectra of freeze-dried calcite crystals, where the samples have been aged in three solutions with different Ca^{2+} concentration over 24 hours, respectively. b-d) XPS photoelectron spectra of freeze-dried calcite crystals, where the sample reached stable in three solutions with different Ca^{2+} concentration over 24 hours b) DI water, c) 3.18 $mg.L^{-1}$ and d) 5.59 $mg.L^{-1}$

We numerically investigate the dynamic distribution of water molecules with calcium ions on the calcite surface by performing the quantum molecular dynamic simulation. The motivation here is to understand the effect of Ca^{2+} on the bound water layer of the calcite surface. The simple model system, which only contains 4 Ca^{2+} ions, cannot be referred to an actual reservoir system. Figure 6(a) shows the time-dependent total energy of the system and Figure 6(b) shows that the snapshots of the water/Ca^{2+}/Calcite system at 2 ps and 4 ps. The system shows that the calcium ions prefer to stay away from the calcite surface to enable water molecules to strongly bind to the calcite surface once the system is heated by the external thermostat. In this region, there exist water molecules with no free ions, which agree with the previous experimentally observation [52, 53]. In the Figure 6(c)& (d), we investigate how water molecules existed on the calcite surface, play a role in determining the calcite surface wettability.

To verify the role of the water layer on the calcite surface in terms of the surface wettability, we perform density functional theory simulation to calculate the adsorption energy of the calcite surface for multiple layers of water through the Young-Dupre equation [39], as given by

$$\cos(\theta) = \frac{U_S^{ad} - U_L^{ad}}{U_L^{ad}} \tag{4}$$

Where U_S^{ad} is the adsorption energy of water molecules on the calcite surface, and U_L^{ad} is the adsorption energy of water molecules on the water covering the calcite surface. Details of adsorption energy calculations can be found in Ref. [54]. Figure 6(c) shows the adsorption energy of each water layer for the underlying calcite surface. For the first layer of water, its adsorption energy on the dry calcite surface is -98 KJ/mol, and for the second and other higher water layers, their adsorption energies on the water covering calcite surface are around -65∼-72 KJ/mol. From the comparison of the adsorption energy, we can find that the binding of the first layer of water to the calcite surface (dry surface) is stronger than those of other water layers to the

wet calcite surface. Then, we can use the Young-Dupre equation to calculate the water contact angle on the calcite surface, which has different layers of water on top of it. Figure 6(d) shows that the DFT-predicted water contact angle increases from 40° to 98°, as the layer number of water is increased from 0 to 1 as shown in Figure 6(d). Then, as the layer number of water is increased, the water contact angle is around 91°. Our calculations suggested that as long as one layer of water is strongly binding to the calcite surface, the predicted WCA is around 91°, which agree with experimental observation. As the Ca^{2+} concentration is low, there is a surface water layer adhering to the calcite surface, as indicated by FTIR and XPS characterization. The top bulk water would mainly interact with the water adsorbed on calcite surface rather than solid calcite surface, which causes the surface to be less adhesive.

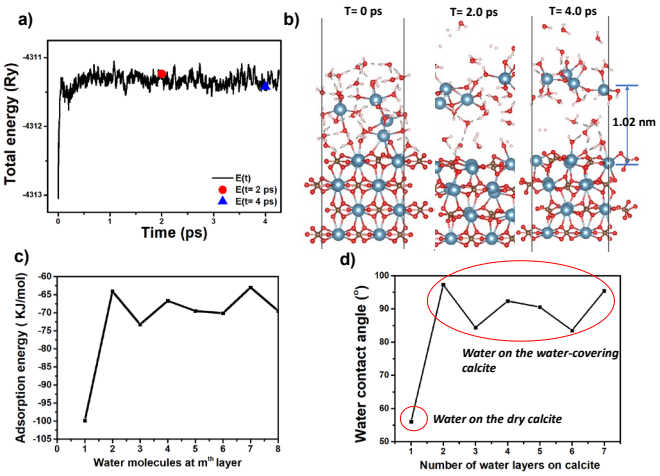

Figure 6 Quantum MD simulation of calcium ionic water on the calcite surface. (a) the total energy of the system versus the time with a time step of 1 fs. (b) snapshot of the calcite/calcium ion water at 0 ps, 2 ps, and 4ps. (c) DFT predicted adsorption energy of water molecules at different water layer on the calcite surface. (d) DFT predicted water contact angle on the calcite surface with a different number of layers through Young-Dupre equation.

Conclusions

In this work, we combined macroscopic, microscopic and nanoscopic analytical techniques, to study the wettability alteration of calcite and addressed its relation to the dissolution process. We have shown that calcite wettability alteration in DI water is caused by the development of chemical heterogeneities identified as strongly adhere water layer to the calcite surface, which causes a change in the surface energy. We have also shown that the chemical heterogeneities are triggered by the dissolution of calcite and depend on the solution saturation state. Upon exposure to the DI water the calcite surface undergoes a transition from super-hydrophilic (SCA = 5°) to hydrophobic (SCA 93° ± 6.4°) within 3 hours. This phenomenon was confirmed using dynamic AFM-based imaging and force reconstruction techniques and the wettability change was proven to be caused by chemical variation rather than morphological changes. The nanoscopic study provided an insight into the progression of chemical heterogenies covering the calcite surface as the system reaches an equilibrium state. The dissolution process was also evaluated by measuring the concentration of Ca^{2+} ions throughout the aging process and it showed a continues increase until the system reached an equilibrium state. We have shown that the water-wetness of the calcite surface is closely linked to both the rate of calcite dissolution and the degree of water saturation. When there is high saturation with Ca^{2+} ions, the dissolution reactions proceed slowly, causing minimal changes to surface wettability. In contrast, lower saturation levels accelerate the dissolution process, resulting in notable alterations to surface wettability. Surface composition analysis along with Quantum MD and density functional theory simulation, showed that at low saturation of Ca^{2+} ions concentration a strong water layer adhering to the calcite surface. Effectively screening the polar interaction of the calcite surface and causing it to be hydrophobic.

Conflicts of interest

The authors declare no competing financial interests.

Acknowledgements

We are grateful to the National Centre for High-performance Computing in Taiwan for computer time and facilities. This work was funded under the Cooperative Agreement between the Khalifa University of Science and Technology, Masdar campus, Abu Dhabi, UAE and the Massachusetts Institute of Technology (MIT), Cambridge, MA, USA, Reference Number FR2017-000001. M.C. acknowledges the support of the Arctic Center for Sustainable Energy (ARC), UiT Arctic University of Norway through Grant No. 310059.

References

1. Buhmann, D. and W. Dreybrodt, *The kinetics of calcite dissolution and precipitation in geologically relevant situations of karst areas: 1. Open system.* Chemical geology, 1985. **48**(1-4): p. 189-211.
2. Arif, M., et al., *CO2 storage in carbonates: Wettability of calcite.* International Journal of Greenhouse Gas Control, 2017. **62**: p. 113-121.
3. Tripathi, R., et al., *Evaluating the role of Salts on Wettability Alteration in Dolomite Rocks: Possibility of Water based Oil Mobilization Application.* Journal of Molecular Liquids, 2023: p. 122738.
4. Xie, Y., M. Khishvand, and M. Piri, *Wettability of calcite surfaces: impacts of brine ionic composition and oil phase polarity at elevated temperature and pressure conditions.* Langmuir, 2020. **36**(22): p. 6079-6088.
5. Li, S., M.D. Jackson, and N. Agenet, *Role of the calcite-water interface in wettability alteration during low salinity waterflooding.* Fuel, 2020. **276**: p. 118097.

6. Rao, A., et al., *Formation and Stability of Heterogeneous Organo–Ionic Surface Layers on Geological Carbonates.* Energy & Fuels, 2022. **36**(14): p. 7414-7433.
7. Stipp, S.L.S., *Toward a conceptual model of the calcite surface: hydration, hydrolysis, and surface potential.* Geochimica et Cosmochimica Acta, 1999. **63**(19): p. 3121-3131.
8. Katende, A. and F. Sagala, *A critical review of low salinity water flooding: Mechanism, laboratory and field application.* Journal of Molecular Liquids, 2019. **278**: p. 627-649.
9. Liu, F. and M. Wang, *Review of low salinity waterflooding mechanisms: Wettability alteration and its impact on oil recovery.* Fuel, 2020. **267**: p. 117112.
10. Nande, S.B. and S.D. Patwardhan, *A review on low salinity waterflooding in carbonates: challenges and future perspective.* Journal of Petroleum Exploration and Production Technology, 2022. **12**(4): p. 1037-1055.
11. Maghsoudian, A., et al., *Direct insights into the micro and macro scale mechanisms of symbiotic effect of SO42−, Mg2+, and Ca2+ ions concentration for smart waterflooding in the carbonated coated micromodel system.* Journal of Molecular Liquids, 2020. **315**: p. 113700.
12. Minde, M.W., et al., *Mineral replacement in long-term flooded porous carbonate rocks.* Geochimica et Cosmochimica Acta, 2020. **268**: p. 485-508.
13. Bahaloo Horeh, M., et al., *Role of brine composition and water-soluble components of crude oil on the wettability alteration of a carbonate surface.* Energy & Fuels, 2019. **33**(5): p. 3979-3988.
14. Al-Bayati, A., et al., *Wettability alteration during low-salinity water flooding.* Energy & Fuels, 2022. **36**(2): p. 871-879.
15. Sloyan, K., et al., *Discerning the Contribution of Morphology and Chemistry in Wettability Studies.* The Journal of Physical Chemistry A, 2018. **122**(38): p. 7768-7773.
16. Zhang, P. and T. Austad, *Wettability and oil recovery from carbonates: Effects of temperature and potential determining ions.* Colloids and Surfaces A: Physicochemical and Engineering Aspects, 2006. **279**(1-3): p. 179-187.
17. HEATH, G.R. and C. CULBERSON, *Calcite: Degree of Saturation, Rate of Dissolution, and the Compensation Depth in the Deep Oceans.* GSA Bulletin, 1970. **81**(10): p. 3157-3160.
18. Decker, D.D., V.J. Polyak, and Y. Asmerom, *Depth and timing of calcite spar and 'spar cave'genesis: Implications for landscape evolution studies.* Caves and karst across time. GSA Special Publication, 2016. **516**: p. 103-111.
19. Stumm, W. and J.J. Morgan, *Aquatic chemistry: chemical equilibria and rates in natural waters*. 2012: John Wiley & Sons.
20. Derkani, M.H., et al., *Mechanisms of Surface Charge Modification of Carbonates in Aqueous Electrolyte Solutions.* Colloids and Interfaces, 2019. **3**(4): p. 62.
21. Wang, J., et al., *Understanding the effects of salinity on bitumen-calcite interactions.* Fuel Processing Technology, 2021. **213**: p. 106668.
22. Palandri, J.L. and Y.K. Kharaka, *A compilation of rate parameters of water-mineral interaction kinetics for application to geochemical modeling*, in *Open-File Report*. 2004.
23. Rao, A., et al., *Nonmonotonic Coupled Dissolution-Precipitation Reactions at the Mineral–Water Interface.* Advanced Functional Materials, 2021. **31**(51): p. 2106396.
24. Al Mahrouqi, D., J. Vinogradov, and M.D. Jackson, *Zeta potential of artificial and natural calcite in aqueous solution.* Advances in colloid and interface science, 2017. **240**: p. 60-76.
25. Jackson, M.D., D. Al-Mahrouqi, and J. Vinogradov, *Zeta potential in oil-water-carbonate systems and its impact on oil recovery during controlled salinity water-flooding.* Scientific reports, 2016. **6**(1): p. 37363.
26. Rao, A., et al., *Nonmonotonic Coupled Dissolution-Precipitation Reactions at the Mineral–Water Interface.* Advanced functional materials, 2021. **31**(51): p. 2106396.
27. Hillner, P., et al., *AFM images of dissolution and growth on a calcite crystal.* Ultramicroscopy, 1992. **42**: p. 1387-1393.
28. Ding, H., S. Mettu, and S. Rahman, *Probing the Effects of Ca2+, Mg2+, and SO42–on Calcite–Oil Interactions by "Soft Tip" Atomic Force Microscopy (AFM).* Industrial & Engineering Chemistry Research, 2020. **59**(29): p. 13069-13078.
29. Al Mahri, M.A., et al., *Surface alteration of calcite: interpreting macroscopic observations by means of AFM.* Physical Chemistry Chemical Physics, 2017. **19**(37): p. 25634-25642.
30. Hu, X.L. and A. Michaelides, *Water on the hydroxylated (0 0 1) surface of kaolinite: From monomer adsorption to a flat 2D wetting layer.* Surface Science, 2008. **602**(4): p. 960-974.
31. Rodriguez-Navarro, C., et al., *Thermal decomposition of calcite: Mechanisms of formation and textural evolution of CaO nanocrystals.* American Mineralogist, 2009. **94**(4): p. 578-593.
32. Karoussi, O., et al., *AFM study of calcite surface exposed to stearic and heptanoic acids.* Colloids and Surfaces A: Physicochemical and Engineering Aspects, 2008. **325**: p. 107-114.
33. Maragliano, C., et al., *Effective AFM cantilever tip size: methods for in-situ determination.* Measurement Science and Technology, 2015. **26**(1): p. 015002.
34. Kiros, A., A. Gholap, and G. Gigante, *Fourier transform infrared spectroscopic characterization of clay minerals from rocks of Lalibela churches, Ethiopia.* International journal of physical sciences, 2013. **8**: p. 109-119.
35. Giannozzi, P., et al., *Advanced capabilities for materials modelling with Quantum ESPRESSO.* Journal of Physics: Condensed Matter, 2017. **29**(46): p. 465901.
36. Limbach, H.J., et al., *ESPResSo—an extensible simulation package for research on soft matter systems.* Computer Physics Communications, 2006. **174**(9): p. 704-727.
37. Hua, X., X. Chen, and W.A. Goddard, *Generalized generalized gradient approximation:An improved density-functional theory for accurate orbital eigenvalues.* Physical Review B, 1997. **55**(24): p. 16103-16109.
38. Vanderbilt, D., *Soft self-consistent pseudopotentials in a generalized eigenvalue formalism.* Physical Review B, 1990. **41**(11): p. 7892-7895.

39. Grimme, S., *Semiempirical GGA-type density functional constructed with a long-range dispersion correction.* Journal of Computational Chemistry, 2006. **27**(15): p. 1787-1799.
40. Martínez, N.F. and R. García, *Measuring phase shifts and energy dissipation with amplitude modulation atomic force microscopy.* Nanotechnology, 2006. **17**(7): p. S167.
41. Teng, H.H., *Controls by saturation state on etch pit formation during calcite dissolution.* Geochimica et Cosmochimica Acta, 2004. **68**(2): p. 253-262.
42. Morse, J.W. and R.S. Arvidson, *The dissolution kinetics of major sedimentary carbonate minerals.* Earth-Science Reviews, 2002. **58**(1): p. 51-84.
43. MacInnis, I.N. and S.L. Brantley, *Development of etch pit size distributions on dissolving minerals.* Chemical Geology, 1993. **105**(1): p. 31-49.
44. Santos, S., *Enhanced sensitivity and contrast with bimodal atomic force microscopy with small and ultra-small amplitudes in ambient conditions.* Applied Physics Letters, 2013. **103**(23).
45. Lai, C.-Y., S. Santos, and M. Chiesa, *Systematic Multidimensional Quantification of Nanoscale Systems From Bimodal Atomic Force Microscopy Data.* ACS Nano, 2016. **10**(6): p. 6265-6272.
46. Lu, J.-Y., et al., *Insights into graphene wettability transparency by locally probing its surface free energy.* Nanoscale, 2019. **11**(16): p. 7944-7951.
47. Israelachvili, J.N., *10 - Unifying Concepts in Intermolecular and Interparticle Forces*, in *Intermolecular and Surface Forces (Third Edition)*, J.N. Israelachvili, Editor. 2011, Academic Press: San Diego. p. 191-204.
48. Chou, L., R.M. Garrels, and R. Wollast, *Comparative study of the kinetics and mechanisms of dissolution of carbonate minerals.* Chemical Geology, 1989. **78**(3): p. 269-282.
49. Batchelor-McAuley, C., et al., *Calcium Carbonate Dissolution from the Laboratory to the Ocean: Kinetics and Mechanism.* Chemistry – A European Journal, 2022. **28**(68): p. e202202290.
50. Ricci, M., et al., *Direct Visualization of Single Ions in the Stern Layer of Calcite.* Langmuir, 2013. **29**(7): p. 2207-2216.
51. Brown, M.A., A. Goel, and Z. Abbas, *Effect of Electrolyte Concentration on the Stern Layer Thickness at a Charged Interface.* Angew. Chem. Int. Ed., 2016. **55**: p. 3790-3794.
52. Lyklema, J., *Fundamentals of interface and colloid science: soft colloids*. Vol. 5. 2005: Elsevier.
53. Grahame, D.C., *The electrical double layer and the theory of electrocapillarity.* Chemical reviews, 1947. **41**(3): p. 441-501.
54. Lu, J.-Y., et al., *The evolution in graphitic surface wettability with first-principles quantum simulations: the counterintuitive role of water.* Physical Chemistry Chemical Physics, 2018. **20**(35): p. 22636-22644.